Supplementary Information for

Room-temperature selective cyclodehydrogenation on Au(111) via radical addition of open-shell resonance structures

Deng-Yuan Li,[1,*] Zheng-Yang Huang,[2] Li-Xia Kang,[2] Bing-Xin Wang,[2] Jian-Hui Fu,[2] Ying Wang,[2] Guang-Yan Xing,[2] Yan Zhao,[2] Xin-Yu Zhang,[2] and Pei-Nian Liu[1,2,*]

[1]School of Pharmacy, China Pharmaceutical University, 211198 Nanjing, P. R. China

[2]School of Chemistry and Molecular Engineering, East China University of Science & Technology, 200237 Shanghai, P. R. China

*E-mail: dengyuanli@cpu.edu.cn, liupn@ecust.edu.cn

Table of contents

Supplementary Note 1. General description

All reactions were carried out in dried glassware under nitrogen atmosphere and anhydrous conditions unless otherwise indicated. Solvents such as dioxane and toluene were distilled from sodium/benzophenone. 1-bromoanthracene-9,10-dione (Purity: >95%), anthracen-2-ylboronic acid (Purity: >95%), carbon tetrabromide (Purity: >95%), $Pd(PPh_3)_4$ (Purity: >95%), and triphenylphosphine (Purity >95%) were purchased from Bide Pharmatech Ltd. Na_2CO_3, DCM, petroleum ether, and ethyl acetate were purchased from Shanghai Titan Scientific Co., Ltd. Reactions were monitored by thin-layer chromatography (TLC) carried out on 0.20 mm Huanghai silica gel plates (HSGF 254) using UV light as the visualizing agent. Products were characterized using ^1H NMR, ^{13}C NMR, and HRMS. NMR spectra were recorded using a Bruker AVANCE III 400 or 600 MHz NMR spectrometer. HRMS were recorded on GCT Premier mass spectrometer (EI, Waters, USA) and Xevo G2 Tof mass spectrometer (ESI, Waters, USA). All ^1H NMR data are reported in δ units, parts per million (ppm), and were calibrated relative to the signals for residual chloroform (7.26 ppm) in deuterochloroform ($CDCl_3$, 99.9% D). All ^{13}C NMR data are reported in ppm relative to $CDCl_3$ (77.16 ppm).

Supplementary Note 2. Synthesis of precursors

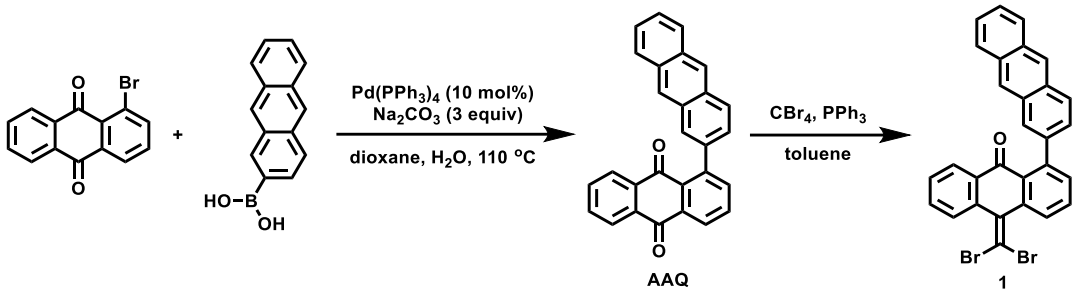

1-bromoanthracene-9,10-dione (190 mg, 0.66 mmol), anthracen-2-ylboronic acid (176 mg, 0.79 mmol), $Pd(PPh_3)_4$ (76.5 mg, 0.066 mmol), and Na_2CO_3 (210 mg, 1.99 mmol) were added in a 25 mL reaction tube under nitrogen atmosphere. After the addition of dioxane (4.5 mL) and H_2O (1.5 mL), the mixture was refluxed for 12 h. The reaction was cooled to room temperature and extracted with DCM. The organic phase was separated and washed with H_2O, and dried over anhydrous Na_2SO_4, filtered, and the solvent was removed in vacuo. The crude product was purified by a preparation plate with silica gel (petroleum ether:EA = 25:1) to afford the [1,2'-bianthracene]-9,10-dione (AAQ, 160 mg, 63%). ^{1}H NMR (600 MHz, $CDCl_3$, 25 °C): δ 8.49 (s, 1H), 8.47 (dd, J_1 = 7.68 Hz, J_2 = 1.2 Hz, 1H), 8.44 (s, 1H), 8.32 (dd, J_1 = 7.68 Hz, J_2 = 1.08 Hz, 1H), 8.12 (dd, J_1 = 7.56 Hz, J_2 = 0.84 Hz, 1H), 8.04 (d, J = 8.64 Hz, 2H), 8.00-8.02 (m, 1H), 7.93 (s, 1H), 7.84 (t, J = 7.56 Hz, 1H), 7.72-7.79 (m, 3H), 7.47-7.50 (m, 2H), 7.38 (dd, J_1 = 8.64 Hz, J_2 = 1.5 Hz, 1H); ^{13}C NMR (150 MHz, $CDCl_3$, 25 °C): δ 183.53, 183.45, 144.45, 139.60, 138.23, 135.08, 134.63, 134.43, 133.91, 133.33, 132.99, 132.11,132.99, 131.81, 131.09, 130.89, 128.38, 128.27, 127.62, 127.52, 127.45, 127.29, 126.96, 126.61, 126.41, 125.97, 125.58, 125.51; HRMS (EI, TOF) m/z: $[M]^+$ calcd for $C_{28}H_{16}O_2$ 384.1150; found 384.1152.

Carbon tetrabromide (156 mg, 0.47 mmol) and triphenylphosphine (247 mg, 0.94 mmol) were added in a 25 mL reaction tube under a nitrogen atmosphere. After the addition of toluene (2 mL), the mixture reacted at 0 °C for 1 h, [1,2'-bianthracene]-9,10-dione (100 mg, 0.26 mmol) was added. The reaction mixture was heated to 80 °C for overnight. The reaction was cooled to room temperature and extracted with DCM. The organic phase was separated and washed with H_2O, and dried over anhydrous Na_2SO_4, filtered, and the solvent was removed in vacuo. The crude product was purified by a preparation plate with silica gel (petroleum ether:EA = 25:1) to afford the desired 10-(dibromomethylene)-[1,2'-bianthracen]-9(10*H*)-one (1, 100 mg, 70%). ^{1}H NMR (400 MHz, $CDCl_3$, 25 °C): δ 8.47 (s, 1H), 8.42 (s, 1H), 8.12 (dd, J_1 = 7.80 Hz, J_2 = 0.84 Hz, 1H), 8.08 (d, J = 7.68 Hz, 1H), 8.00-8.04 (m, 3H), 7.91 (s, 1H), 7.86 (d, J = 7.52 Hz, 1H), 7.59 (t, J = 7.72 Hz, 1H), 7.54 (dt, J_1 = 7.84 Hz, J_2 = 1.4 Hz, 1H), 7.43-7.48 (m, 4H), 7.36-7.38 (m, 1H); ^{13}C NMR (150 MHz, $CDCl_3$, 25 °C): δ 186.23, 142.60, 139.13, 138.67, 137.45, 137.32, 134.68, 132.61, 132.07, 132.03, 131.70, 130.94, 130.71, 130.67, 130.26, 128.89, 128.38, 128.34, 128.28, 127.91, 127.03, 126.96, 126.59, 126.32, 126.30, 125.50, 125.35, 93.65; HRMS (EI, TOF) m/z: $[M]^+$ calcd for $C_{29}H_{16}Br_2O$ 537.9568, 539.9547, 541.9527; found 537.9564, 539.9550, 541.9532.

^{1}H NMR (600 MHz, $CDCl_3$) spectrum of [1,2'-bianthracene]-9,10-dione (AAQ)

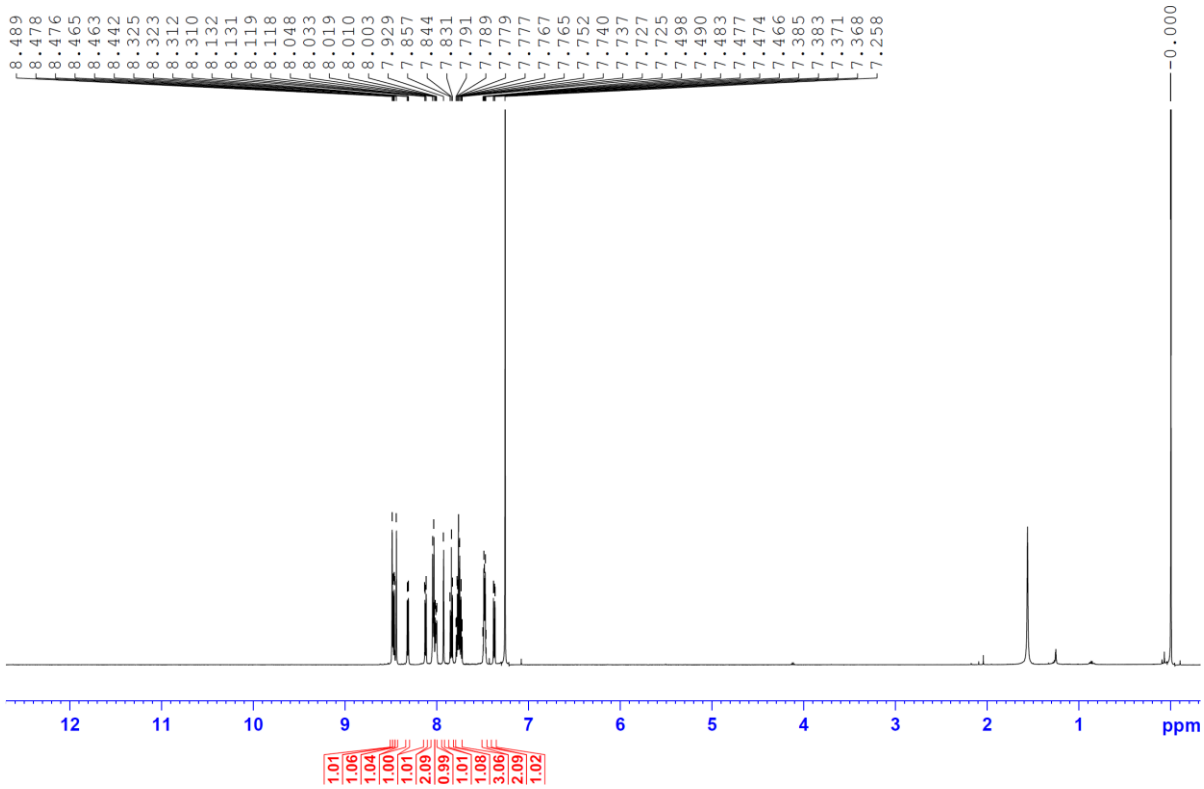

^{13}C NMR (150 MHz, $CDCl_3$) spectrum of [1,2'-bianthracene]-9,10-dione (AAQ)

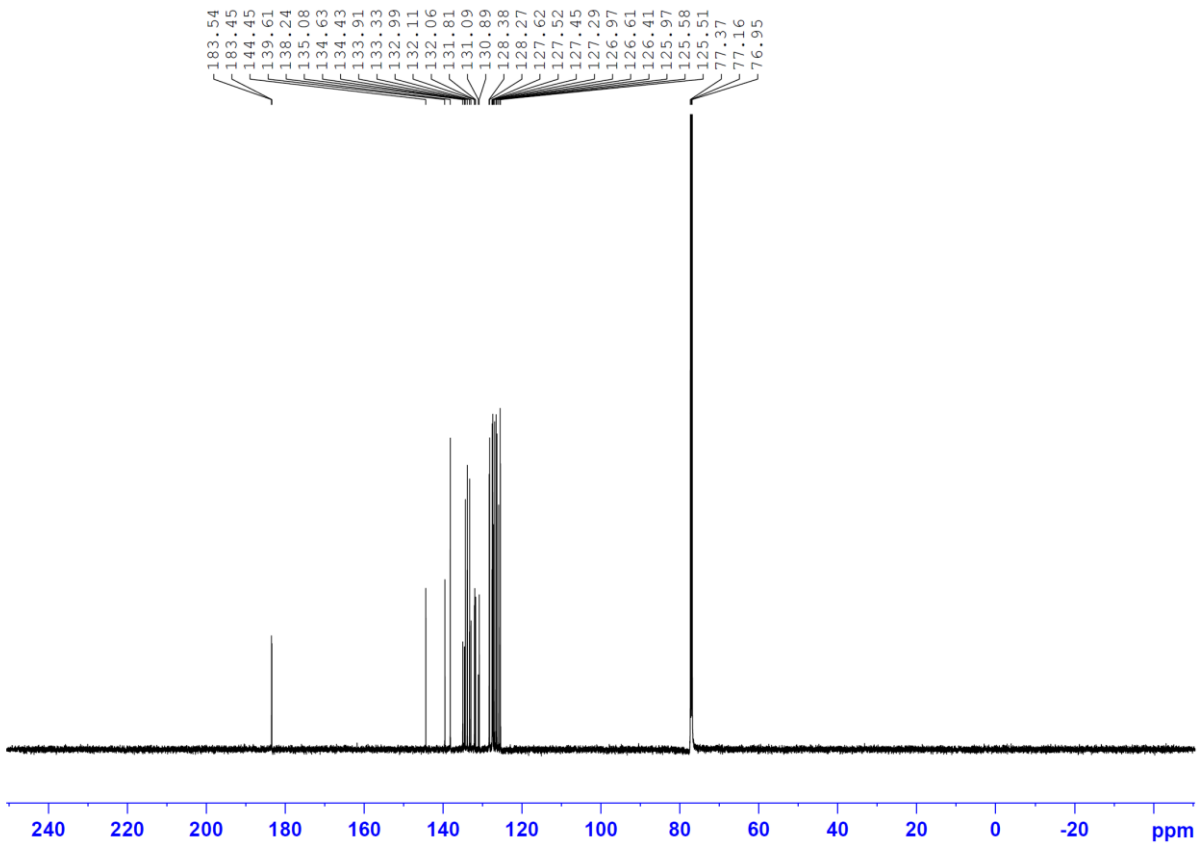

^{1}H NMR (400 MHz, $CDCl_3$) spectrum of 10-(dibromomethylene)-[1,2'-bianthracen]-9(10*H*)-one (1)

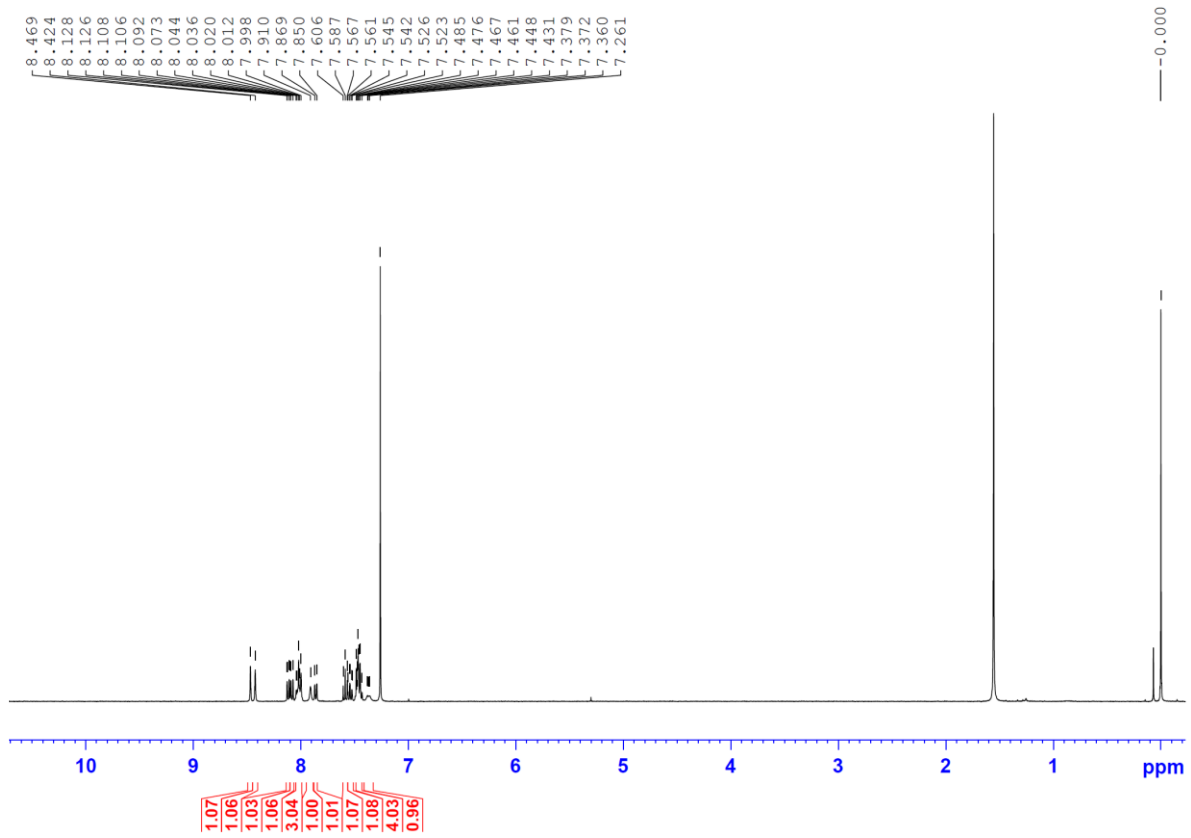

^{13}C NMR (150 MHz, $CDCl_3$) spectrum of 10-(dibromomethylene)-[1,2'-bianthracen]-9(10*H*)-one (1)

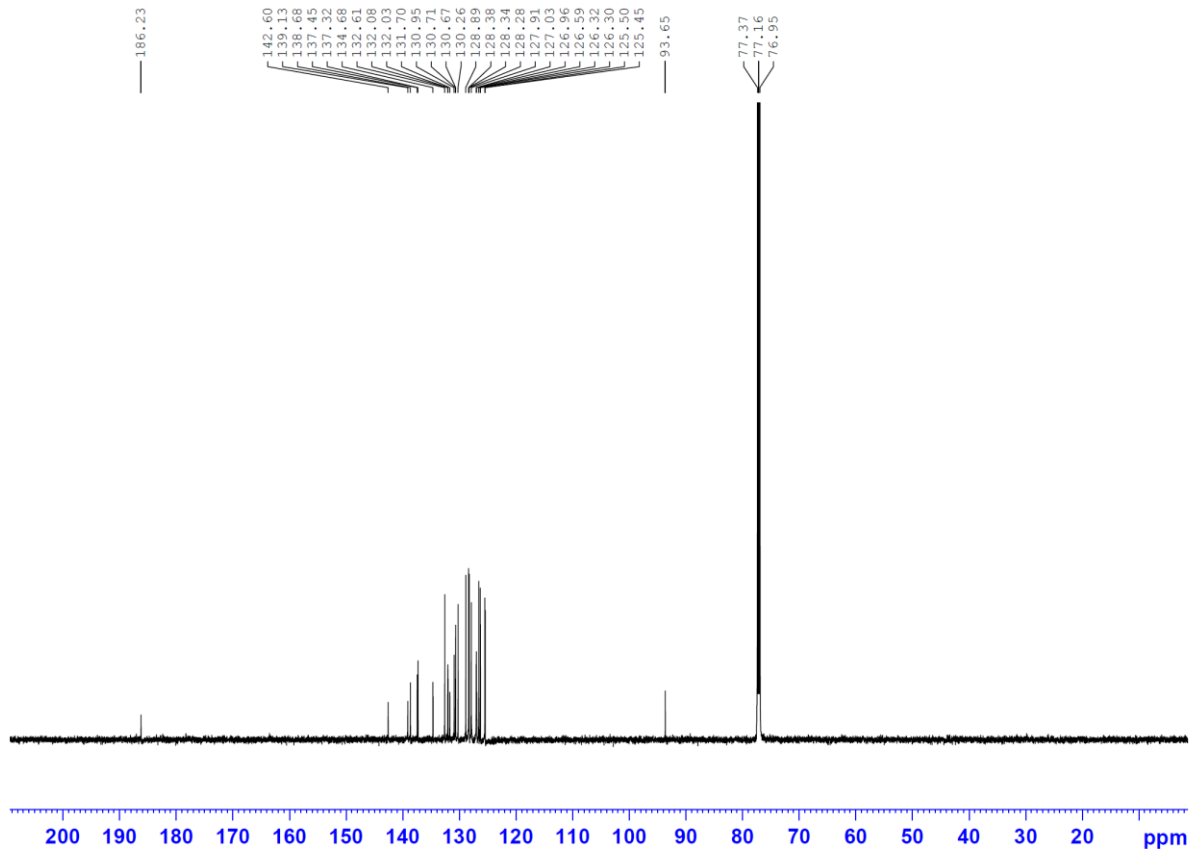

Supplementary Note 3. Room-temperature selective cyclodehydrogenation on Au(111)

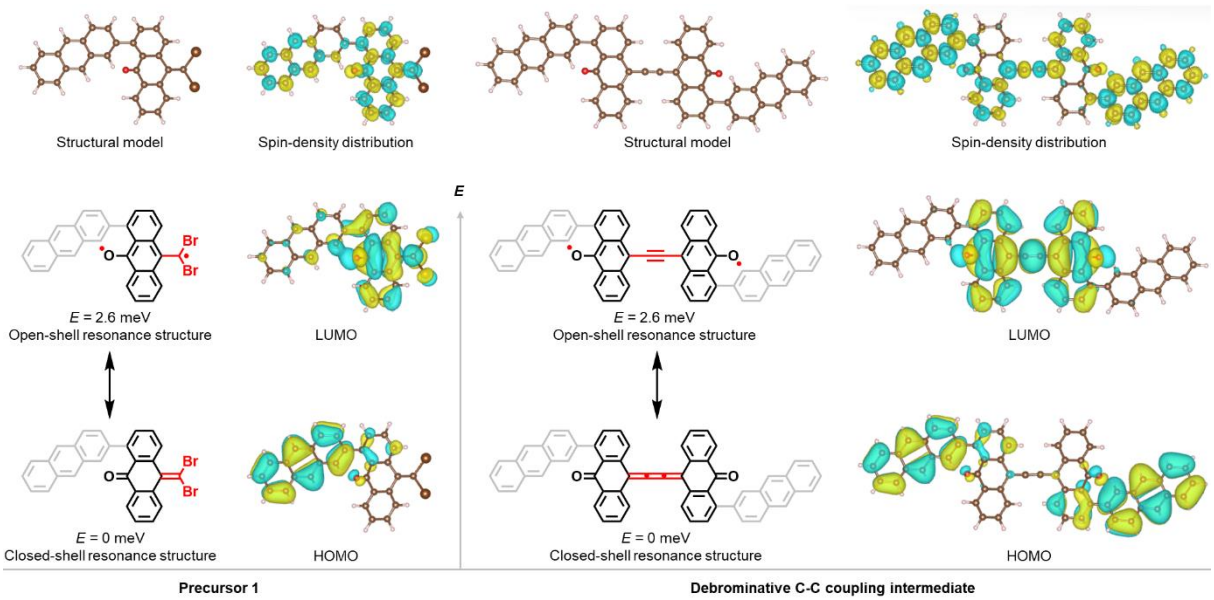

Supplementary Fig. 1 | DFT-calculated relative energies, spin-density distributions (Yellow and green isosurface colors in open-shell resonance structures indicate spin up and spin down, respectively), and frontier molecular orbitals (Yellow and green isosurface colors in closed-shell resonance structures indicate opposite phases of the wave function) of precursor 1 and debrominative C-C coupling intermediate. The structures of precursor 1 and debrominative C-C coupling intermediate were subjected to single point energy calculations by Gaussian 16, Revision A.03[1]. Single point energy calculations used the PBE0-D3(BJ) functional combined with the def2-TZVP basis set[2,3]. Molecular orbitals and electron spin densities were analyzed by Multiwfn[4]. Images of the structures and isosurfaces were plotted using VESTA[5].

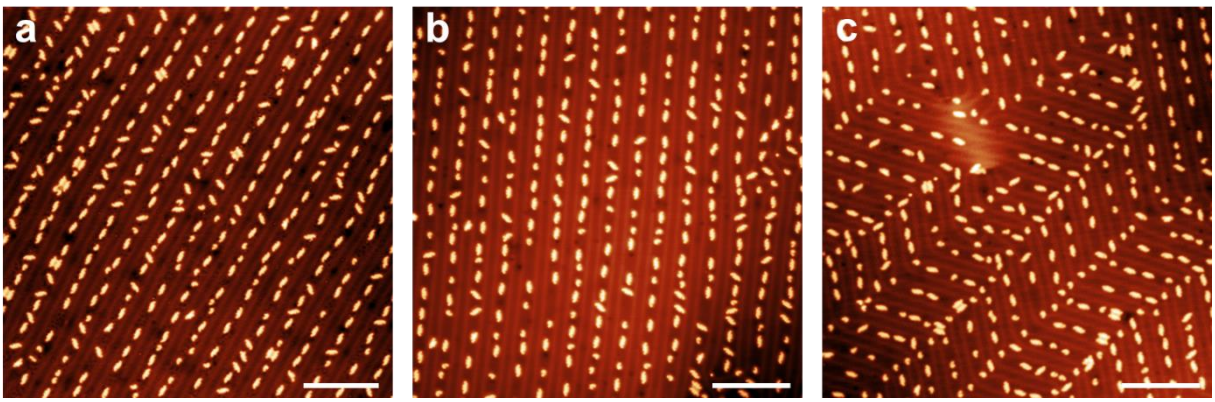

Supplementary Fig. 2 | a-c Large-scale STM images at three different sites after annealing at room temperature for 12 h. Scale bars: 20 nm. Scanning parameters: **a-c** U = 0.5 V, I = 10 pA.

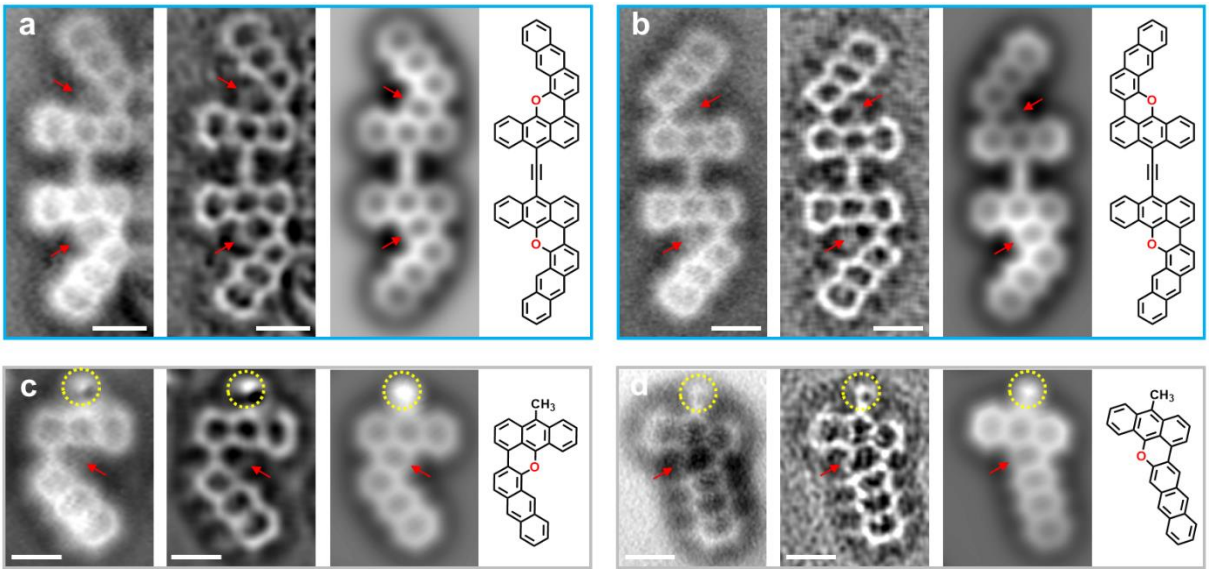

Supplementary Fig. 3 | a,b nc-AFM images of two representative planar dimers formed by the removal of *α*-H and the corresponding Laplace-filtered images, nc-AFM simulations, and chemical structures. **c**,**d** nc-AFM images of two representative planar monomers (**c**: *cis*-monomer; **d**: *trans*-monomer) and the corresponding Laplace-filtered images, nc-AFM simulations, and chemical structures. The red arrows and yellow dotted circles indicate O atoms and methyl groups. The nc-AFM simulations were performed with the probe particle model (https://github.com/ProkopHapala/ProbeParticleModel/wiki)[6,7]. Scale bars of all images: 0.5 nm.

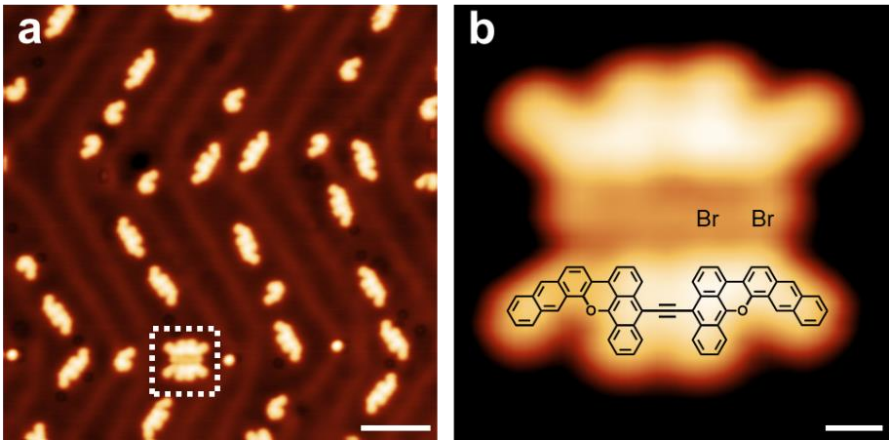

Supplementary Fig. 4 | a High-resolution STM image after annealing at room temperature for 12 h. **b** Zoom-in STM image of the assembly of two planar *cis*-α,α-dimers and bromide atoms (white dotted frame). Scale bars: **a** 5 nm. **b** 0.5 nm. Scanning parameters: **a,b** U = 0.2 V, I = 10 pA.

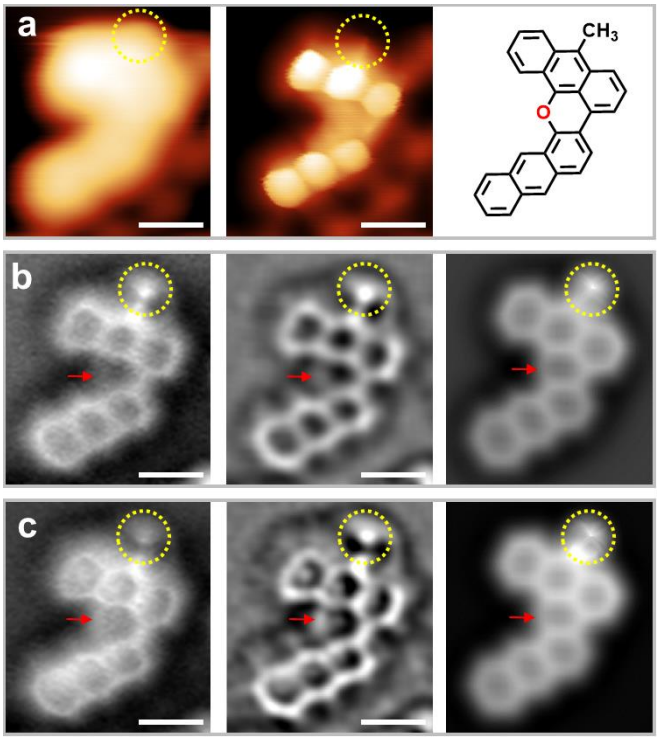

Supplementary Fig. 5 | a Zoom-in STM and BR-STM of one planar *cis*-monomer and the corresponding chemical structure. **b**,**c** nc-AFM images of one planar *cis*-monomer with different tip heights using a flexible CO tip and the corresponding Laplace-filtered images, nc-AFM simulations. The yellow dotted circles and red arrows indicate methyl groups and O atoms. The nc-AFM simulations were performed with the probe particle model (https://github.com/ProkopHapala/ProbeParticleModel/wiki)[6,7]. Scale bars for all images: 0.5 nm. Scanning parameters: **a** STM: U = 50 mV, I = 100 pA. BR-STM: CO tip, constant height, U = 10 mV. Tip height: **b** z = −68 pm with respect to STM setpoint of 0.1 V, 50 pA on Au(111). **c** z = −75 pm with respect to STM setpoint of 0.1 V, 50 pA on Au(111).

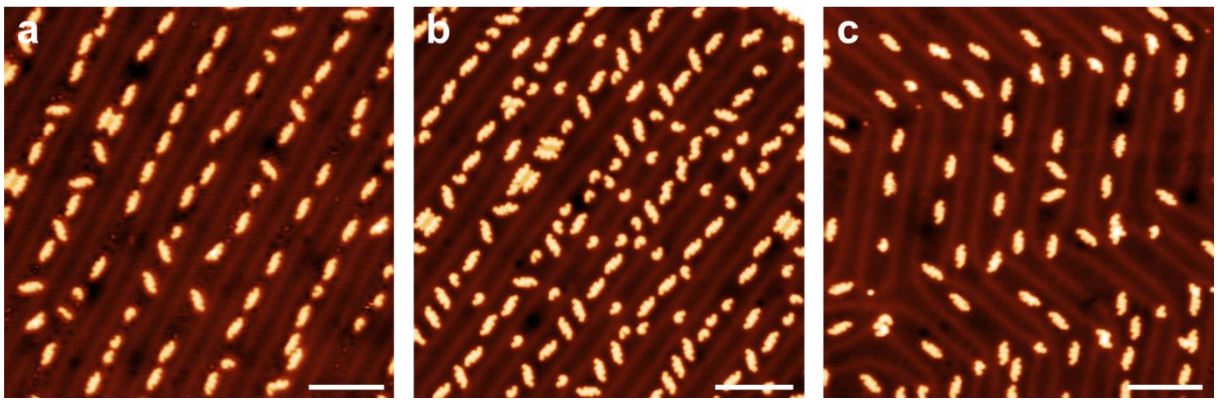

Supplementary Fig. 6 | a-c Large-scale STM image after annealing at the indicated temperatures and times (**a**: 300 K, 12 h; **b**: 333 K, 15 minutes; **c**: 543 K, 15 minutes). Scale bars: 10 nm. Scanning parameters: **a**, **b** U = 0.5 V, I = 10 pA. **c** U = 0.2 V, I = 10 pA.

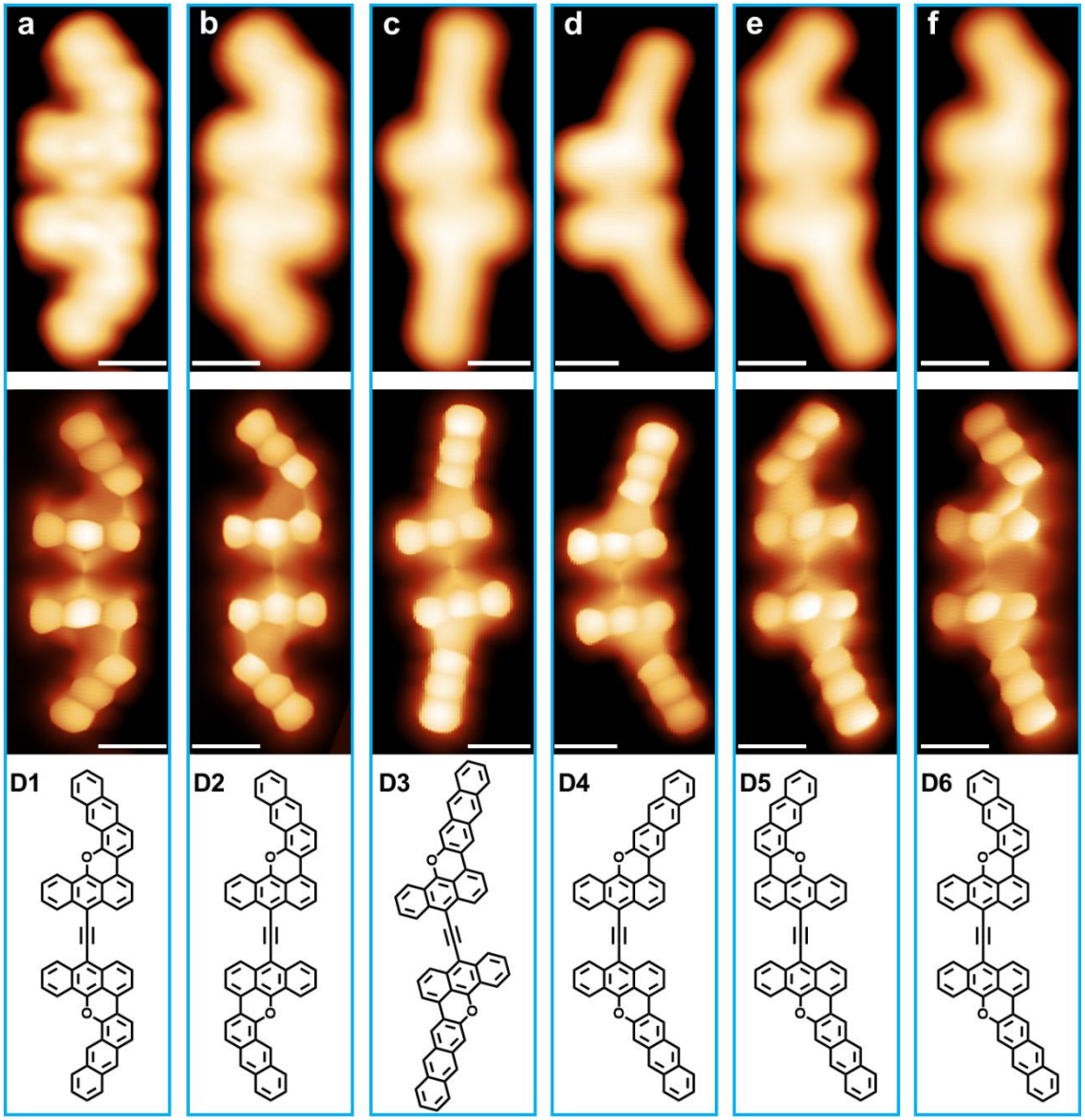

Supplementary Fig. 7 | a-f Amplified (up) and bond-resolved (down) STM images of six observed planar oxa-nanographene products (D1-D6) with different geometries on Au(111) and the corresponding chemical structures. Scale bars: 0.5 nm. Scanning parameters: **a** U = 10 mV, I = 50 pA. **b** U = 50 mV, I = 0.5 nA. **c** U = 0.1 V, I = 50 pA. **d** U = 10 mV, I = 50 pA. **e** U = 0.1 V, I = 30 pA. **f** U = 0.2 V, I = 30 pA. Bond-resolved STM images: CO tip, constant height, **a, e, f** 10 mV, **b-d** 20 mV

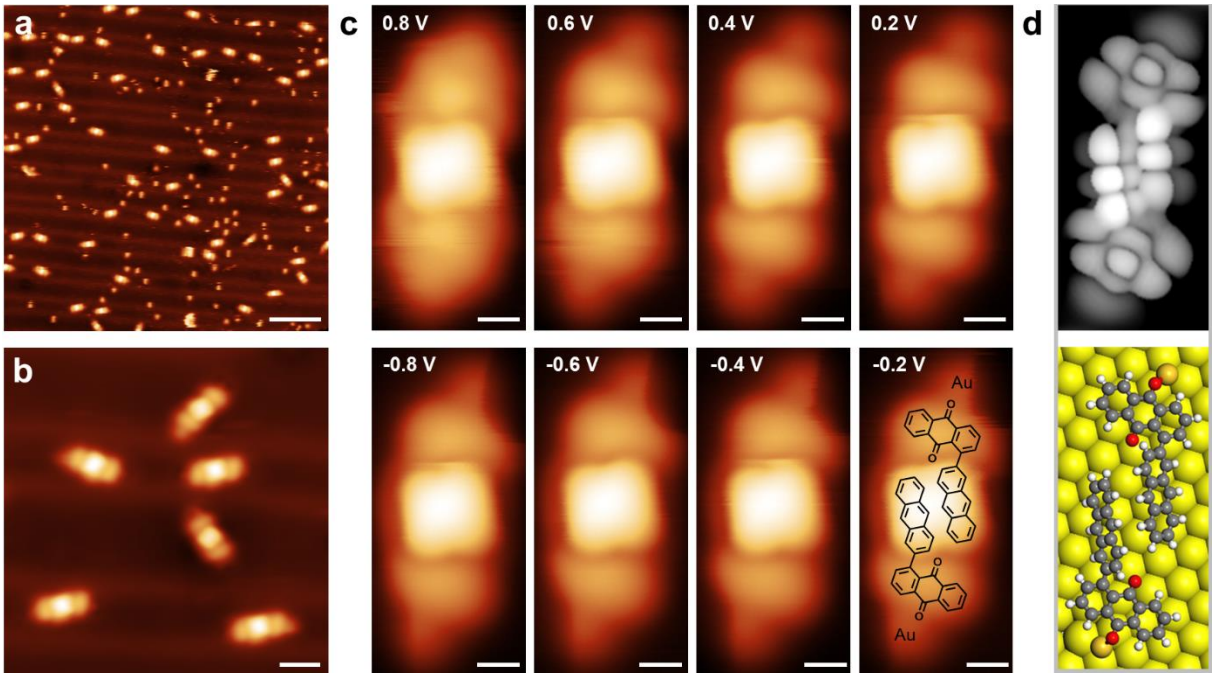

Supplementary Fig. 8 | a Large-scale and **b** high-resolution STM images after dosing AAQ on Au(111) held approximately 300 K. **c** Bias-dependent STM images of a self-assembled dimer composed of two nonplanar AAQ molecules and two Au adatoms and **d** the corresponding STM simulation and structural model. The STM simulation in Supplementary Fig. 8d was performed with the Tersoff-Hamman method[8]. Scale bars: **a** 10 nm. **b** 2 nm. **c** 0.5 nm. Scanning parameters: **a** U = -0.5 V, I = 50 pA. **b** U = -0.5 V, I = 10 pA. **c** U = the indicated voltage in the corresponding STM images, I = 10 pA.

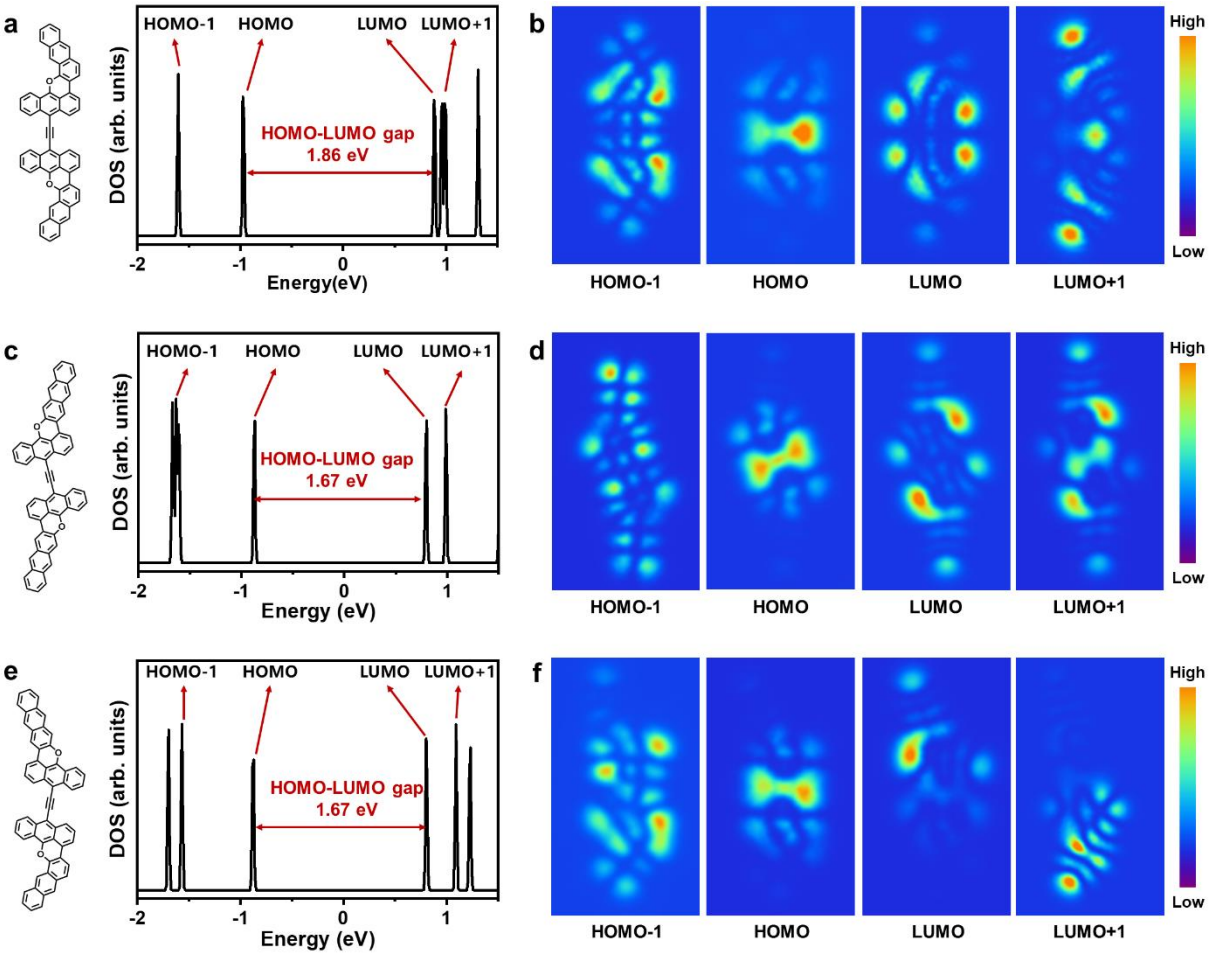

Supplementary Fig. 9 | a, **c**, **e** Chemical structures, DFT-calculated density of states of three representative planar oxa-nanographene products and **b**, **d**, **f** the corresponding simulated LDOS maps of HOMO-1, HOMO, LUMO, and LUMO+1 (HSE06 results[9], see detailed settings in Methods). The Fermi level is set to zero.

Supplementary Note 4. Mechanism of room-temperature selective cyclodehydrogenation on Au(111)

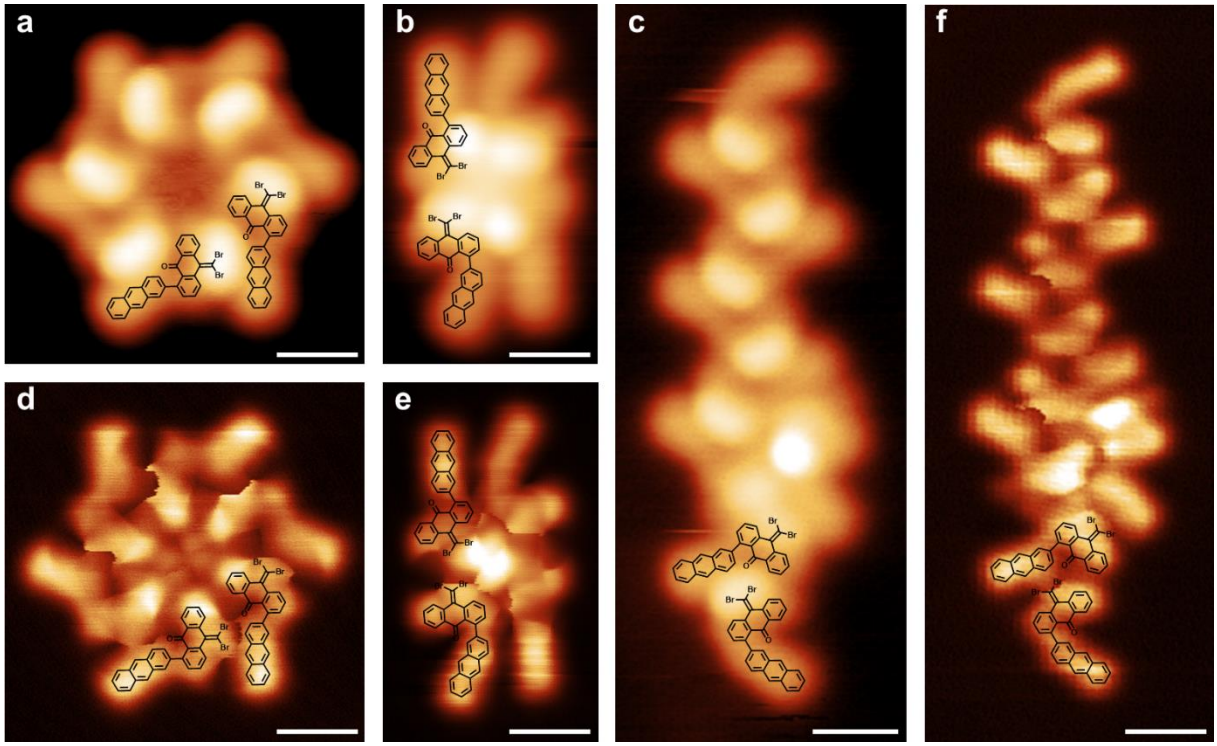

Supplementary Fig. 10 | a-c Amplified STM and **d-f** constant-height current images of three representative aggregates after depositing precursor **1** onto a cold Au(111). **a**,**d** Self-assembled hexamer. **b**,**e** Self-assembled tetramer. **c**,**f** Self-assembled short chain. Scale bars: **a**, **c**, **d**, **f** 1 nm. **b**, **e** 0.5 nm. Scanning parameters: **a**, **b** U = 1 V, I = 10 pA. **c** U = 1.2 V, I = 5 pA. **d-f** CO tip, constant-height, 10 mV.

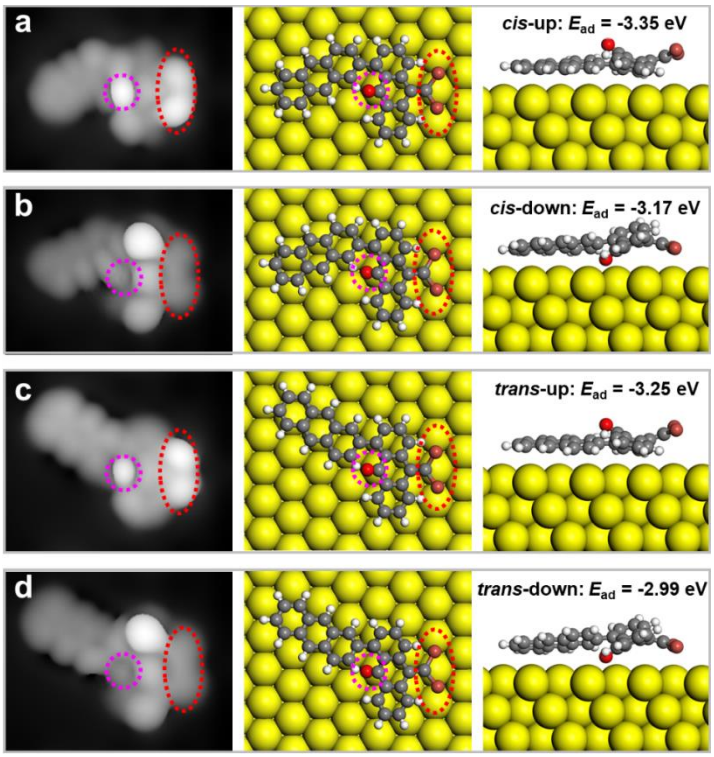

Supplementary Fig. 11 | a-d STM simulations based on DFT-optimized models and the corresponding adsorption energies of precursor **1** with four types of adsorption geometries (**a**: *cis*-up; **b**: *cis*-down; **c**: *trans*-up; **d**: *trans*-down) on Au(111). The STM simulations in Supplementary Fig. 11 were performed with the Tersoff-Hamman method[8].

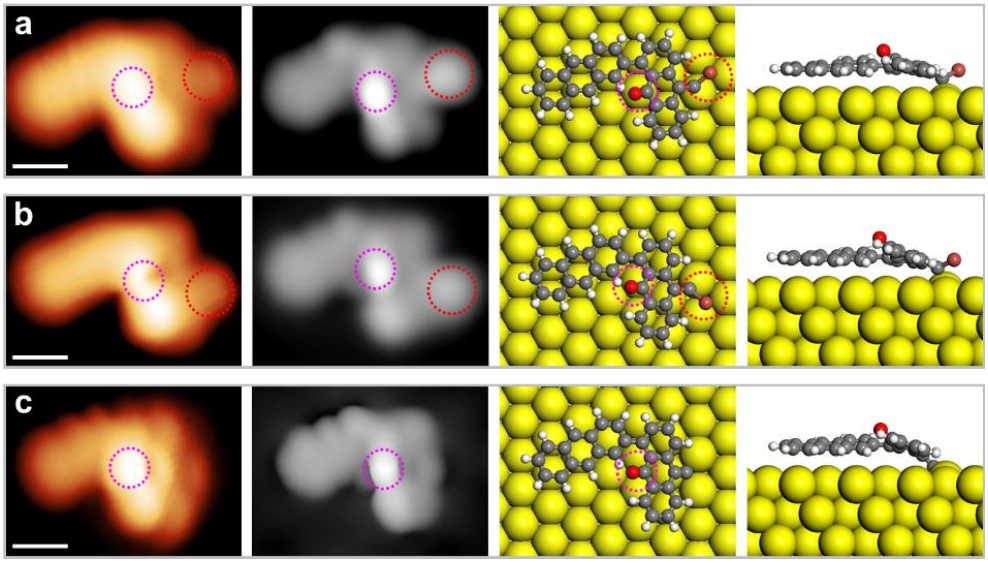

Supplementary Fig. 12 | a-c Amplified STM image and STM simulation of three surface-bound debrominated intermediates formed after removing one or two bromines on Au(111), and the corresponding structure models. The red and pink dotted circles indicate the Br atoms and carbonyl groups, respectively. Scale bars: 0.5 nm. Scanning parameters: **a** U = 0.1 V, I = 10 pA. **b** U = 10 mV, I = 10 pA. **c** U = 50 mV, I = 100 pA. The STM simulations in Supplementary Fig. 12 were performed with the Tersoff-Hamman method[8].

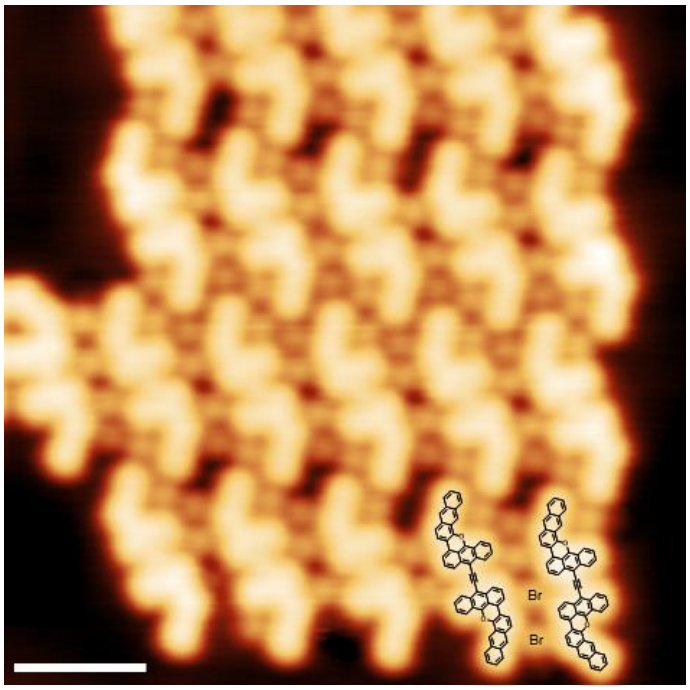

Supplementary Fig. 13 | Molecular islands assembled from planar dimers with bromine atoms on Au(111). Scale bar: 2 nm. Scanning parameter: U = 10 mV, I = 10 pA.

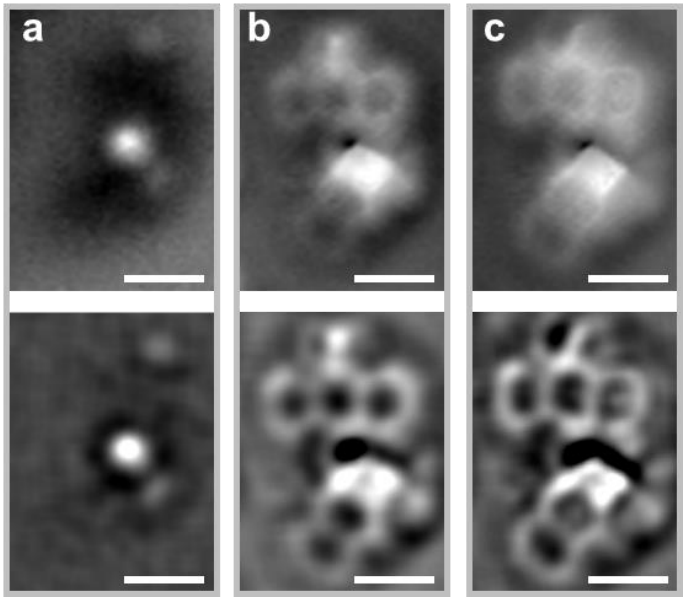

Supplementary Fig. 14 | a-c nc-AFM images (above) of an individual nonplanar monomer species I with different tip heights using a flexible CO tip and the corresponding Laplace-filtered images (below). Scale bars for all images: 0.5 nm. Tip height: **a** z = −18 pm with respect to STM setpoint of 0.1 V, 100 pA on Au(111). **b** z = −32 pm with respect to STM setpoint of 0.1 V, 100 pA on Au(111). **c** z = −89 pm with respect to STM setpoint of 0.1 V, 100 pA on Au(111).

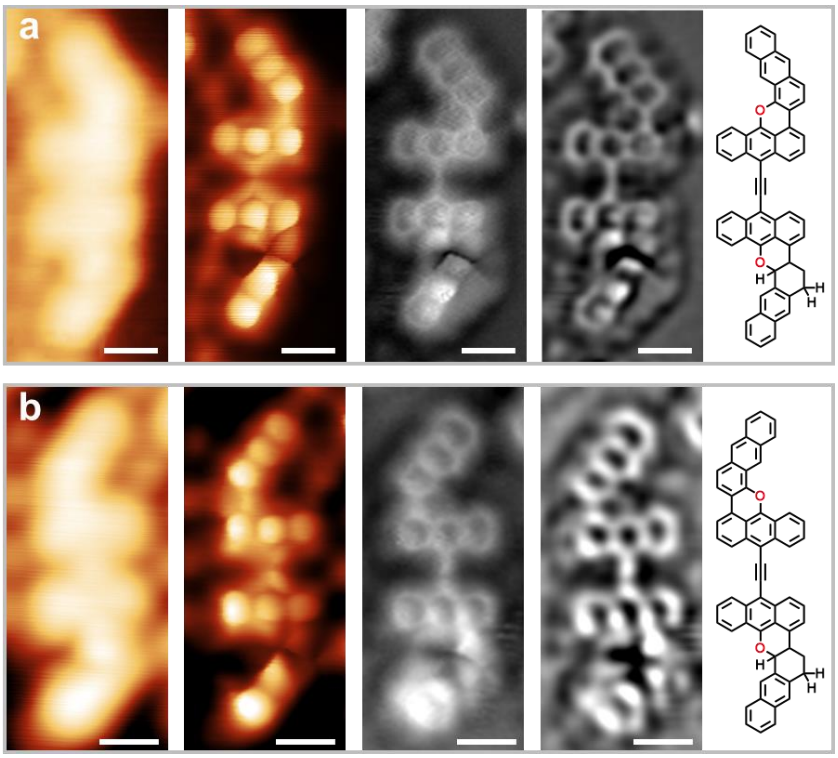

Supplementary Fig. 15 | a Zoom-in STM, BR-STM, and nc-AFM images of nonplanar *cis*-α,α-dimer species II with incomplete dehydrogenation on one side and the corresponding Laplace-filtered nc-AFM image and chemical structure. **b** Zoom-in STM, BR-STM, and nc-AFM images of nonplanar *trans*-α,α-dimer species II with incomplete dehydrogenation on one side and the corresponding Laplace-filtered nc-AFM image and chemical structure. Scale bars for all images: 0.5 nm. Scanning parameters: **a** STM: U = 0.1 V, I = 10 pA. BR-STM: CO tip, constant-height, 10 mV. **b** STM: U = 0.1 V, I = 100 pA. BR-STM: CO tip, constant-height, 10 mV.

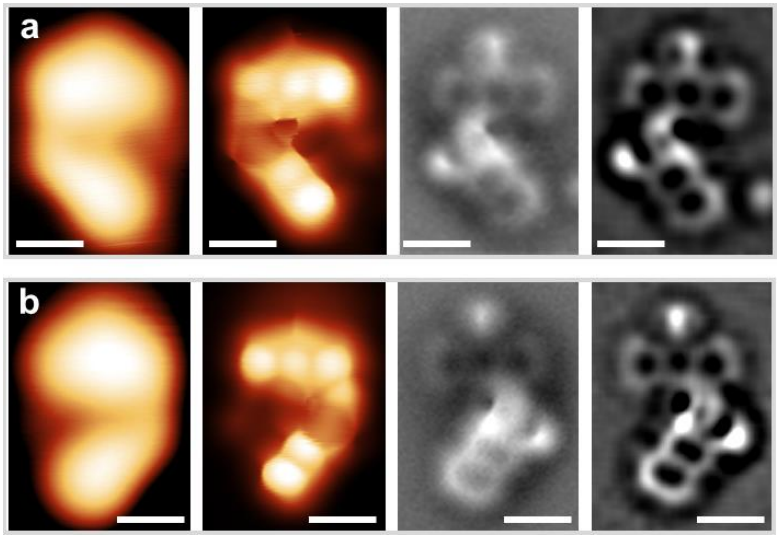

Supplementary Fig. 16 | a,b Zoom-in STM, BR-STM, and **c** nc-AFM images of other nonplanar monomer species and the corresponding Laplace-filtered nc-AFM images. Scale bars for all images: 0.5 nm. Scanning parameters: **a** STM: U = 0.2 V, I = 10 pA. BR-STM: CO tip, constant-height, 10 mV. **b** STM: U = 0.5 V, I = 10 pA. BR-STM: CO tip, constant-height, 10 mV.

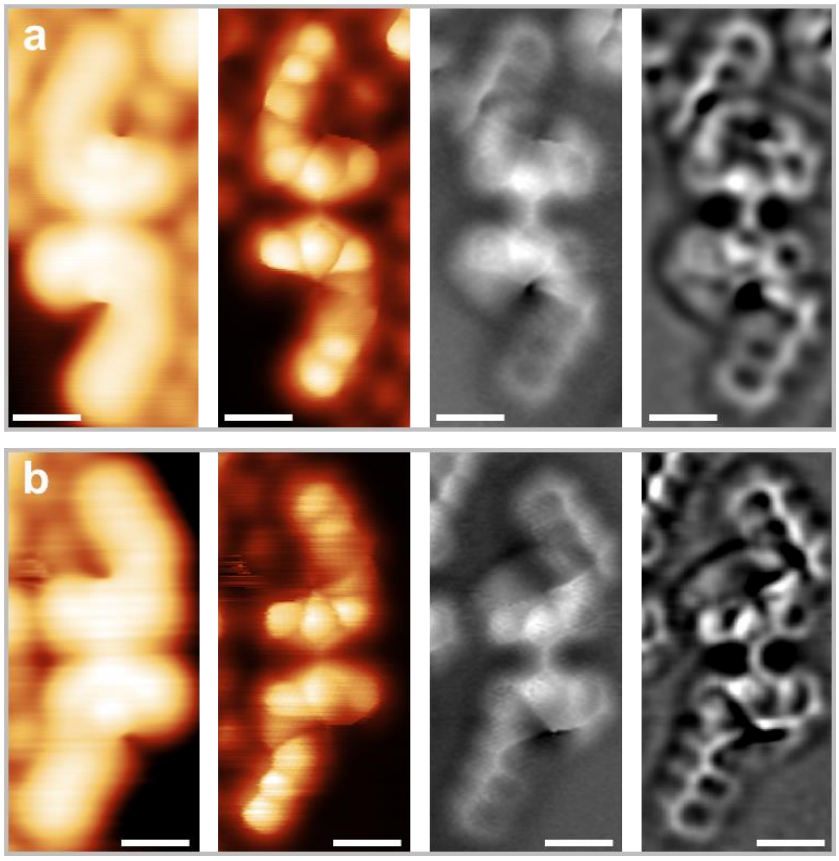

Supplementary Fig. 17 | a,b Zoom-in STM, BR-STM, and **c** nc-AFM images of other nonplanar α,α-dimer and α,β-dimer species and the corresponding Laplace-filtered nc-AFM images. Scale bars for all images: 0.5 nm. Scanning parameters: **a,b** STM: U = 0.1 V, I = 100 pA. BR-STM: CO tip, constant-height, 10 mV.

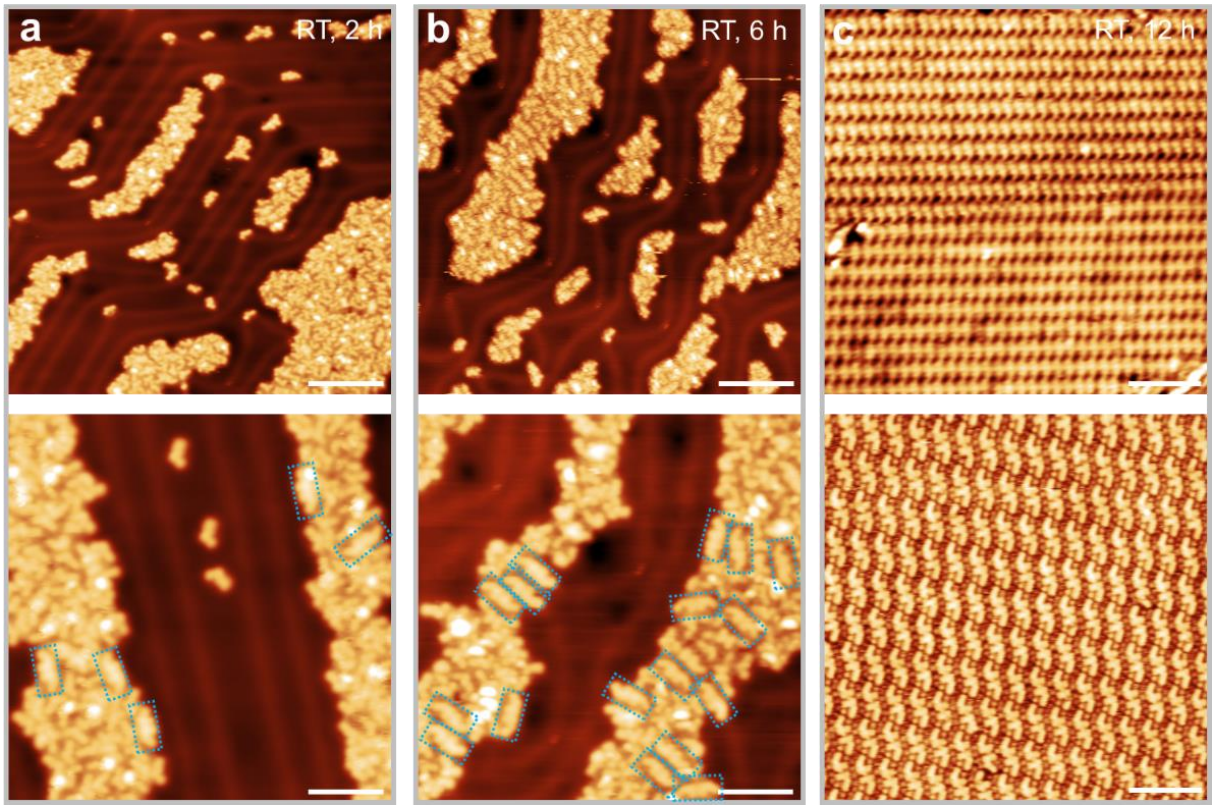

Supplementary Fig. 18 | a-c Large-scale (above:) and high-resolution (below) STM images after annealing a cold Au(111) sample with high coverage precursor **1** at room temperature for the evaluated times. The blue dotted frames indicate the planar dimer products. Scale bars: **a-c** above: 10 nm. below: 5 nm. Scanning parameters: **a** above: U = 1 V, I = 100 pA. below: U = 0.5 V, I = 100 pA. **b** above: U = 0.3 V, I = 100 pA. below: U = 0.2 V, I = 100 pA. **c** above: U = 0.5 V, I = 100 pA. below: U = 10 mV, I = 100 pA.

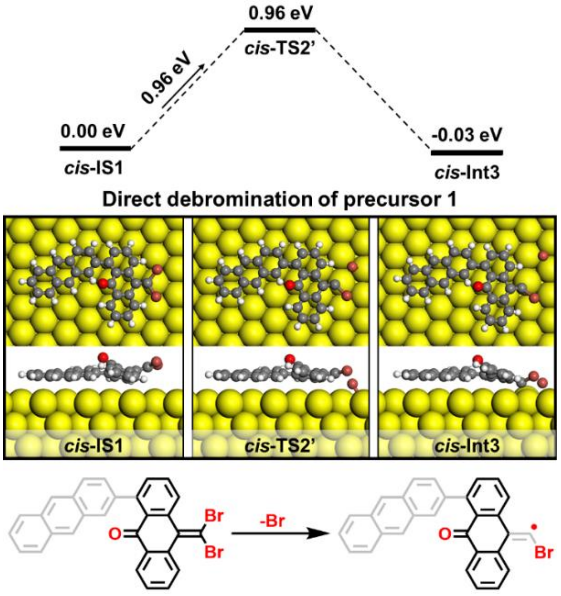

Supplementary Fig. 19 | DFT-calculated direct debromination process of precursor **1** with *cis*-up adsorption geometry. The corresponding calculated molecular structures including top and side views of the initial (IS), transition (TS), and intermediate (Int) states of the reactions are shown below the energy diagrams (CI-NEB method[10], see detailed settings in Methods). The reaction pathways of chemical structures are shown below the molecular structure models (The gray chemical structure represents the part of the molecule closer to the Au(111) surface).

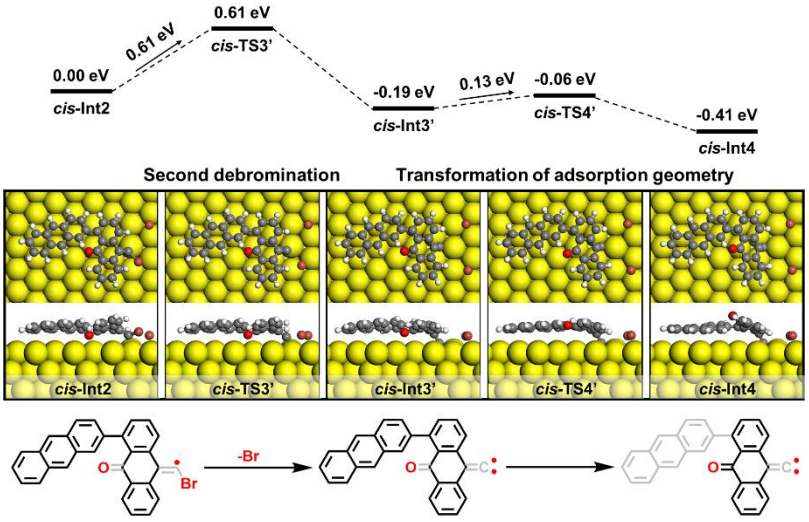

Supplementary Fig. 20 | DFT-calculated the second debromination of *cis*-Int2 followed by an adsorption geometry transformation to form *cis*-Int4. The corresponding calculated molecular structures including top and side views of the initial (IS), transition (TS), and intermediate (Int) states of the reactions are shown below the energy diagrams (CI-NEB method[10], see detailed settings in Methods). The reaction pathways of chemical structures are shown below the molecular structure models (The gray chemical structure represents the part of the molecule closer to the Au(111) surface).

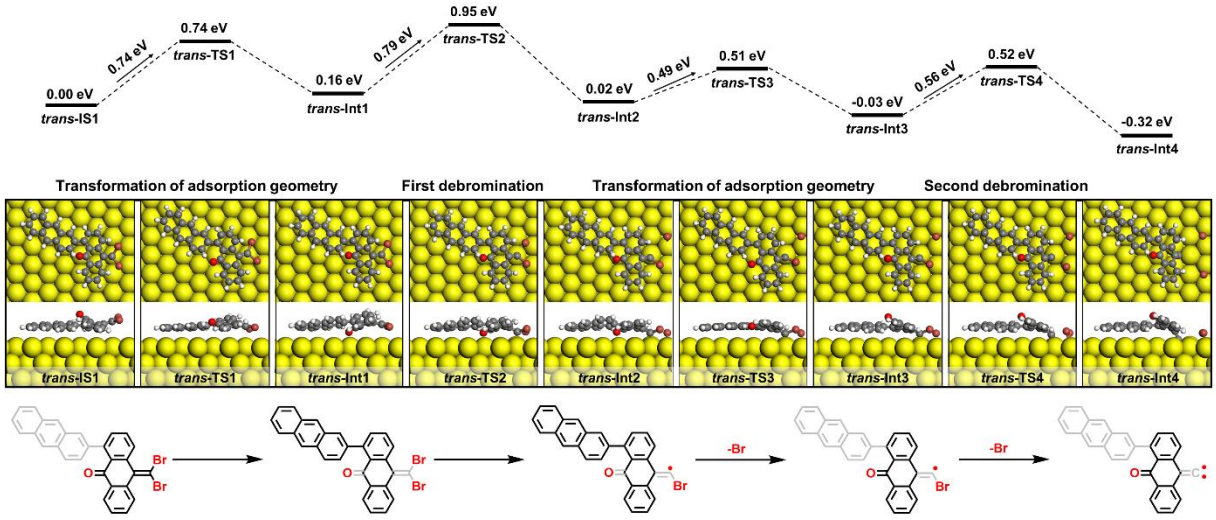

Supplementary Fig. 21 | DFT-calculated indirect debromination process from *trans*-IS1 to *trans*-Int4. The corresponding calculated molecular structures including top and side views of the initial (IS), transition (TS), and intermediate (Int) states of the reactions are shown below the energy diagrams (CI-NEB method[10], see detailed settings in Methods). The reaction pathways of chemical structures are shown below the molecular structure models (The gray chemical structure represents the part of the molecule closer to the Au(111) surface).

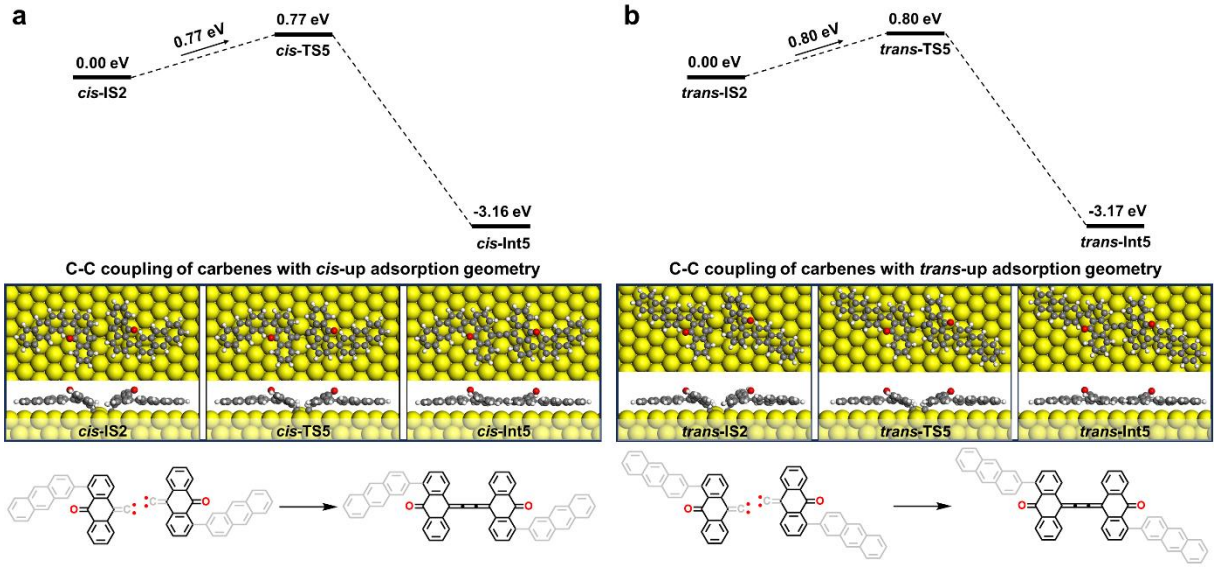

Supplementary Fig. 22 | a, **b** DFT-calculated C-C coupling processes of carbenes with *cis*-up or *trans*-up adsorption geometries. The corresponding calculated molecular structures including top and side views of the initial (IS), transition (TS), and intermediate (Int) states of the reactions are shown below the energy diagrams (CI-NEB method[10], see detailed settings in Methods). The reaction pathways of chemical structures are shown below the molecular structure models (The gray chemical structure represents the part of the molecule closer to the Au(111) surface).

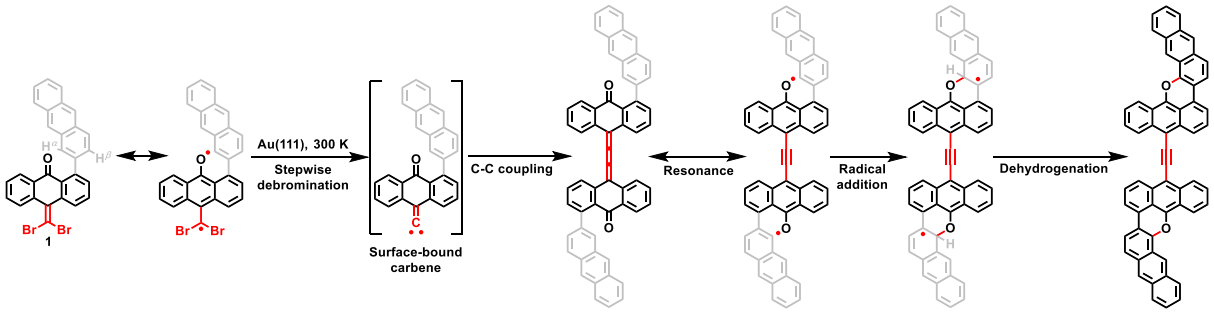

Supplementary Fig. 23 | Proposed cascade reaction pathway involving debromination coupling and cyclodehydrogenation on Au(111) at room temperature.

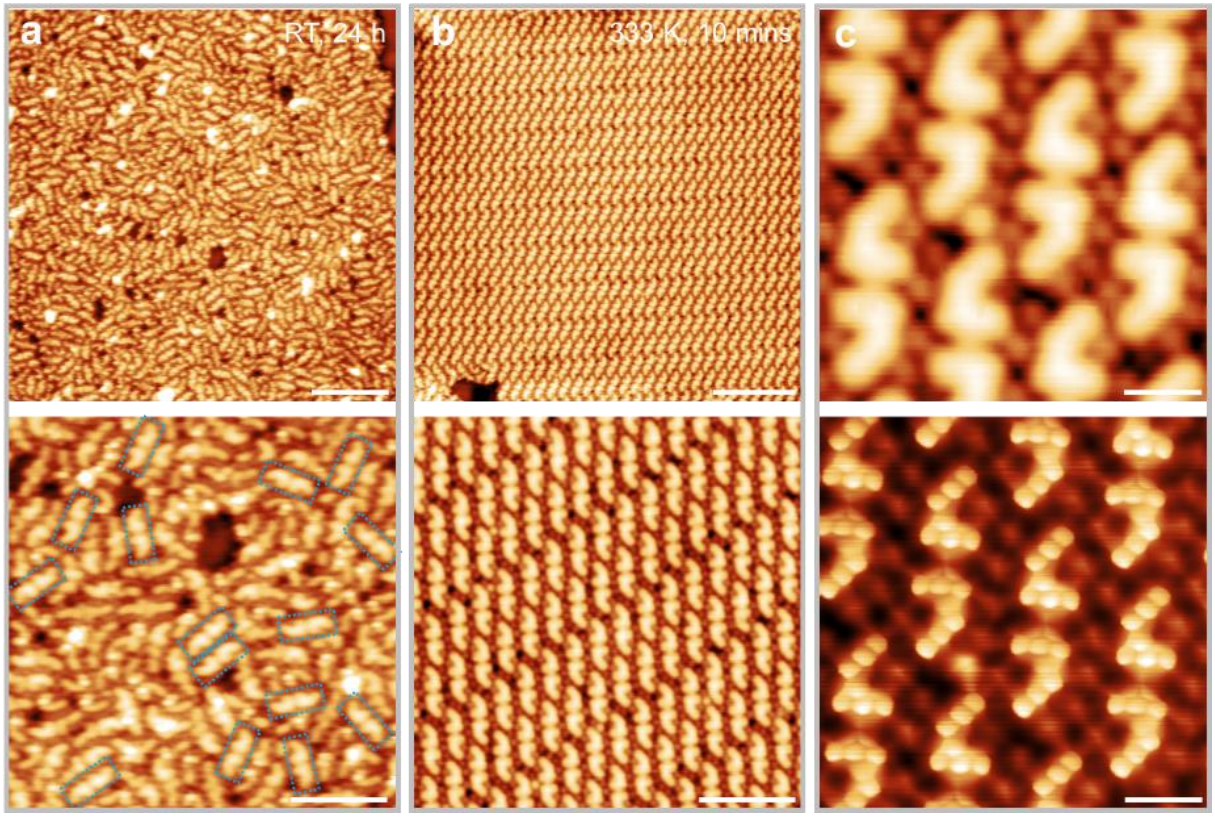

Supplementary Fig. 24 | a Large-scale (above) and high-resolution (below) STM images after annealing a Ag(111) sample with precursor **1** at room temperature for 24 h. The blue dotted frames indicate the planar dimer products. **b** Large-scale (above) and high-resolution (below) STM images after annealing a Ag(111) sample with precursor **1** at 333 K for 10 minutes. **c** Zoom-in STM (above) and BR-STM (below) images of planar dimer products on Ag(111). Scale bars: **a,b** above: 10 nm. below: 5 nm. **c** 1 nm. Scanning parameters: **a** U = 0.1 V, I = 10 pA. **b** U = 10 mV, I = 10 pA. **c** above: U = 10 mV, I = 10 pA. below: CO tip, constant height, U = 10 mV.

Supplementary References

1. Frisch, M. J. et al. Gaussian, Inc., Wallingford CT, 2016.
2. Grimme, S., Antony, J., Ehrlich, S. & Krieg, H. A consistent and accurate ab initio parametrization of density functional dispersion correction (DFT-D) for the 94 elements H-Pu. *J. Chem. Phys.* **132**, 154104 (2010).
3. Weigend, F. & Ahlrichs, R. Balanced basis sets of split valence, triple zeta valence and quadruple zeta valence quality for H to Rn: Design and assessment of accuracy. *Phys. Chem. Chem. Phys.* **7**, 3297–3305 (2005).
4. Lu, T. & Chen, F. Multiwfn: A multifunctional wavefunction analyzer. *J. Comput. Chem.* **33**, 580–592 (2012).
5. Momma, K. & Izumi, F. VESTA 3 for three-dimensional visualization of crystal, volumetric and morphology data. *J. Appl. Crystallogr.* **44**, 1272–1276 (2011).
6. Jel ínek, P. High resolution SPM imaging of organic molecules with functionalized tips. *J. Phys.: Condens. Matter* **29**, 343002 (2017).
7. Hapala, P., Ondráček, M. M., Stetsovych, O., Švec, M. & Jelínek, P. Simultaneous nc-AFM/STM Measurements with Atomic Resolution. (Berlin: Springer) ch. **3**, pp 29–49 (2015).
8. Tersoff, J. & Hamann, D. R. Theory and Application for the Scanning Tunneling Microscope. *Phys. Rev. Lett.* **50**, 1998 (1983).
9. Paier, J. et al. Screened hybrid density functionals applied to solids. *J. Chem. Phys.* **124**, 154709 (2006).
10. Henkelman, G. & J ónsson, H. A climbing image nudged elastic band method for finding saddle points and minimum energy paths. *J. Chem. Phys.* **113**, 9901–9904 (2000).